Research Article

Novel Chitosan Polymer Design, Synthesis Using *Mentha piperita* of ZnO NPs as a Catalyst: Antibacterial Evaluation against Gram-Negative Multidrug-Resistant Pathogens

Ponnusamy Packialakshmi,[1] **Perumal Gobinath,**[1] **Daoud Ali,**[2] **Saud Alarifi** [iD],[2]
Balasubramani Ravindran,[3] **Akbar Idhayadhulla** [iD],[1]
and Radhakrishnan Surendrakumar [iD] [1]

[1]*PG & Research, Department of Chemistry, Nehru Memorial College (Affiliated Bharathidasan University), Puthanamapatti, South, Tamilnadu, India*
[2]*Department of Zoology, College of Science, King Saud University, P.O. Box 2455, Riyadh 11451, Saudi Arabia*
[3]*Department of Environmental Energy and Engineering, Kyonggi University, Yeongtong-gu, Suwon, Gyeonggi-Do 16227, Republic of Korea*

Correspondence should be addressed to Akbar Idhayadhulla; a.idhayadhulla@gmail.com
and Radhakrishnan Surendrakumar; surendrakumar@nmc.ac.in

The goal of this research is to create a novel Schiff base of chitosan polymer derivatives 1a-1j. Nanotechnology is a promising field since it avoids the usage of hazardous chemicals while also saving time. Using the leaf extract of the pharmacologically valuable herb *Mentha piperita*, we described a green synthesis of ZnO NPs. Zinc oxide ions may be easily reduced into ZnO NPs using a *Mentha piperita* extract. ZnO NPs were employed as a phytocatalyst in this investigation to make chitosan derivatives. The synthetic procedure is straightforward, with a short reaction time and a high yield. Our newly synthesized compounds have been characterized by FTIR and nuclear magnetic resonance spectroscopy (^{1}H NMR and ^{13}C NMR), and morphology analysis was observed by XRD, SEM, and TEM. In addition, the antibacterial activity was also evaluated against gram-positive bacteria and gram-negative bacteria. Compound 1b is extremely active against gram-negative bacteria (4.0 μg/mL, *E. coli*), and compound 1h is highly active against gram-positive bacteria (6.0 μg/mL, *S. aureus*) compared with standard erythromycin and other chitosan derivatives. As a result, compounds 1b and 1h could be a high crucial molecule in the development of antibacterial drugs.

1. Introduction

Antibacterial activity of biopolymers has been broadly studied for the last years. The (CH) (-1-4)-d-glucosamine) is the deacetylated structure of chitin, which is extracted from natural and marine animals [1, 2]. Chitin can be isolated from microorgans [3], crustacean [4], and bug [5]. Chitin deacetylation improves its solubility in acid medium while additionally increasing its antibacterial motion [6, 7]. Antimicrobial resistance is one of the third most serious concerns affecting human health, according to the WHO [8]. Recent studies have combined antibacterial nanoparticles with chitosan-linked ZnO composites, which have shown to have good antibacterial properties [9]. Chitosan, an adaptable hydrophilic polysaccharide derived from chitin, has a vast antibacterial range, making it prone to each

gram-negative and gram-positive microorganism [10]. The biopolymer is widely employed in bioinformatics applications as a drug transporter [11], antibacterial [12], antioxidant [13], anticancer [14], and wound dressing agent [15, 16] due to its unique qualities such as harmless, antibacterial activity, decomposable, and high biocompatibility [17, 18]. Over the last decade, nanomedicine has developed rapidly, and it now provides promising treatments for bacterial infections. Because nanoparticles behave differently from their parent bulk, nanotechnology opens up new possibilities for medicinal applications [19–22]. The size and size distribution of nanoparticles, as well as their composition, shape, surface charge, surface chemistry, and surface functionalization, hydrophobicity, crystalline phase, crystallite size, and porosity, are all important factors that influence the physicochemical properties and, as a result, the activity of nanomaterials [23, 24]. Nanoparticles with antibacterial properties can act as antibacterial agents or transporters, increasing antibiotic bioavailability and effectiveness [25]. Metallic nanoparticles, primarily composed of zinc, silver, or copper, have been found to have potent antibacterial properties [26]. The antibacterial drug was prepared using low cost, environmental friendliness, synthesizability in ambient atmosphere, and nontoxicity. A recent study has shown that green synthesis is the most effective method for synthesizing NPs [27]. Furthermore, ZnO NP is being used in biological and environmental sectors such as pharmaceutical administration, biological sensing, biological labelling, gene transfer, and nanomedicine [28–31]. ZnO NPs have also been reported to have antibacterial, antifungal, acaricidal, prediculicidal, and larvicidal properties [32–36]. Chitosan and its derivatives are referred to as ecological cleansing useful resources because they efficiently restrict the growth and reproduction of harmful bacteria as well as poisonous contaminants [37]. Physicochemical and biochemical features of chitosan derivatives include good antimicrobial activity, hygroscopic, and embolism. As a result, it has potential uses in a variety of disciplines, including agriculture, medicines, cosmetics, food processing, environmental protection, and biotechnology [38–47]. The chitosan molecule's containing enormous number of primary amine and hydroxyl groups allows for a wide range of chemical changes, resulting in a new class of biomaterials [48]. Chemical modifications to chitosan, such as sulfonation [49], amination [50], and carboxymethylation [51], allow for chemical transformation of the NH_2 and OH groups and the creation of different functional derivatives. Modified diisocyanate has been shown to have increased antibacterial activity [52–57]. The antibacterial activity of chitosan derivatives is shown in Figure 1. Similarly, the important functional groups in chitosan can readily react with amine groups to generate the appropriate chitosan Schiff base with imine characteristic group (-RC=N-). Chitosan Schiff base derivatives are one of the finest possibilities for improving antibacterial activity of chitosan [58]. Based on the above literature report, all the research work was done by using several amines but none of the researchers are not using the ethylenediamine react with C-2 position in chitosan, Schiff base formation in C-5 position, and green catalyst of ZnO NPs was used for our

research work. The present work addresses the development of antibacterial aminoethyl chitosan derivatives and was characterized by Fourier transform infrared (FT-IR) and nuclear magnetic resonance (^{1}H NMR and ^{13}C NMR) spectroscopy, and morphology and its physical properties were observed by TEM, SEM, and X- ray diffraction (XRD). Additionally, their antibacterial activity was evaluated against a various pathogenic microorganisms.

2. Materials and Methods

2.1. General Methods. All the chemicals and reagents such as chitosan (degree of deacetylation—75%, Mw141 kDa), acetic acid, EDA, aromatic aldehydes, ethanol, and DMF are bought from Sigma Aldrich, India. Melting points of synthesized compounds were recorded in open capillary tubes and are uncorrected. On a Shimadzu 8201pc (4000–1000 cm^{-1}), the FT-IR spectra were captured using the kBr disc approach. A Bruker DRX-300 MHz was used to record the ^{1}H NMR and ^{13}C NMR spectra. To obtain NMR spectra, the compound was dissolved in DMSO-d$_6$. The morphology of zinc oxide nanoparticles is confirmed by using XRD, SEM, and TEM. The scanning electron microscope (SEM) model VP-1450 (LEO, Co., Germany), was used for SEM analysis. For transmission electron microscopy (TEM) analysis, an LEO 912 AB instrument was used. TLC was used to assess the purity of the compounds, with silica-gel as the adsorbent and 60F254 aluminium sheets as the adsorbent, and it was visualized by ultraviolet (E-Series UV hand lamp (254/365 nm wave length)).

2.1.1. Swelling Test of Chitosan Polymer. The bulge properties of the chitosan derivative were investigated in various media. Preweighted derivative samples (0.05 g for each test) were immersed in 35 mL 0.20 M acetic acid, 0.20 M HCl, water, and 0.20 M NaOH, respectively [59]. The samples were withdrawn from the media, wiped with filter paper, and weighted once they had reached equilibrium swelling (1 day). Each sample's swelling ratio was calculated using the following equation:

$$\text{Swelling ratio}(\%) = \left(W_t - \frac{W_0}{W_0} \right) \times 100\%, \qquad (1)$$

where W_t and W_0 represent the weight of the swollen and dry samples, respectively.

2.2. Preparation of Mentha piperita Leaf Extract. 5 grams of *Mentha piperita* leaves was rinsed thoroughly with distilled water and sanitized with alcohol using a delicate scouring technique. These leaves were warmed in 100 mL of distilled water at 60°C for 45 minutes. After that, Whatman 41 filter paper was used to sieve the extract. A cool and dry place was used to store the filtrate.

2.2.1. Synthesis of Zinc Oxide Nanoparticles. 20 mL *Mentha piperita* leaf extract was mixed with 60 mL 20 percent NaOH solution to make zinc oxide nanoparticles via precipitation reaction procedure. Then, in a 250 ml measuring glass, 5 mL portions of that combination and 60 ml refined water
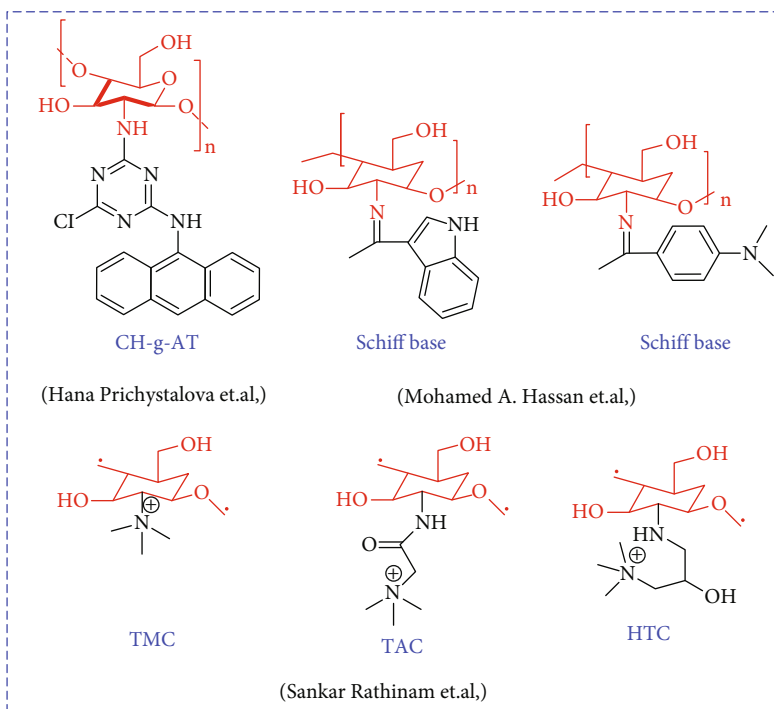
FIGURE 1: The antibacterial activity of chitosan derivatives.

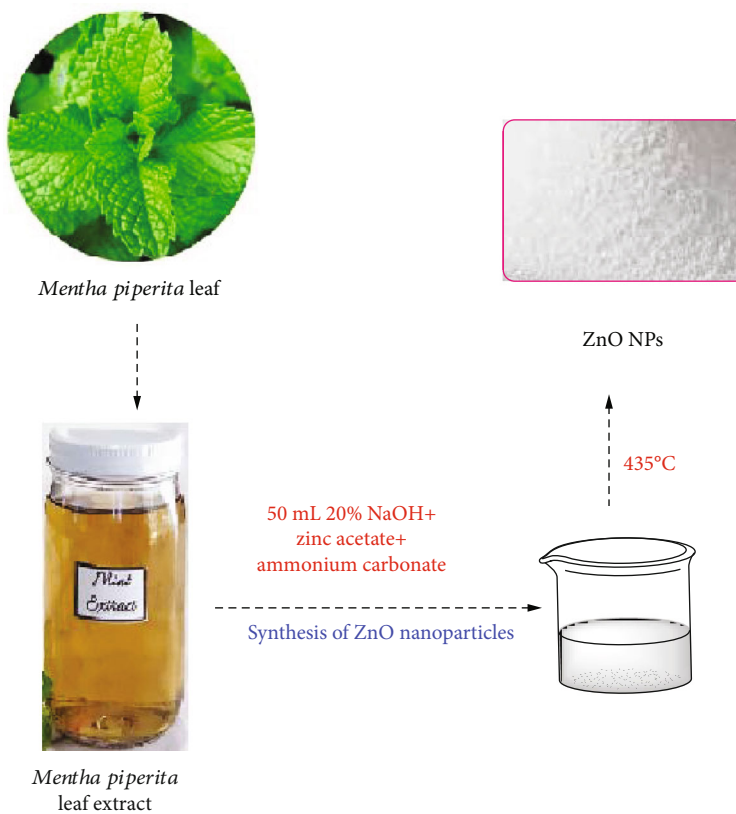FIGURE 2: Synthesis of ZnO nanoparticles from *Mentha piperita*.

were added and blended for 1.5 hours. Then, with steady mixing, zinc acetate (2.1 g in 100 ml water) and ammonium carbonate (0.95 g in 100 ml) solutions were added drop by drop into the measuring glass. After the reaction was completed, the suspension was mixed at 750 rpm for 1 hour at 30°C. Finally, the precipitate was filtered and rinsed with
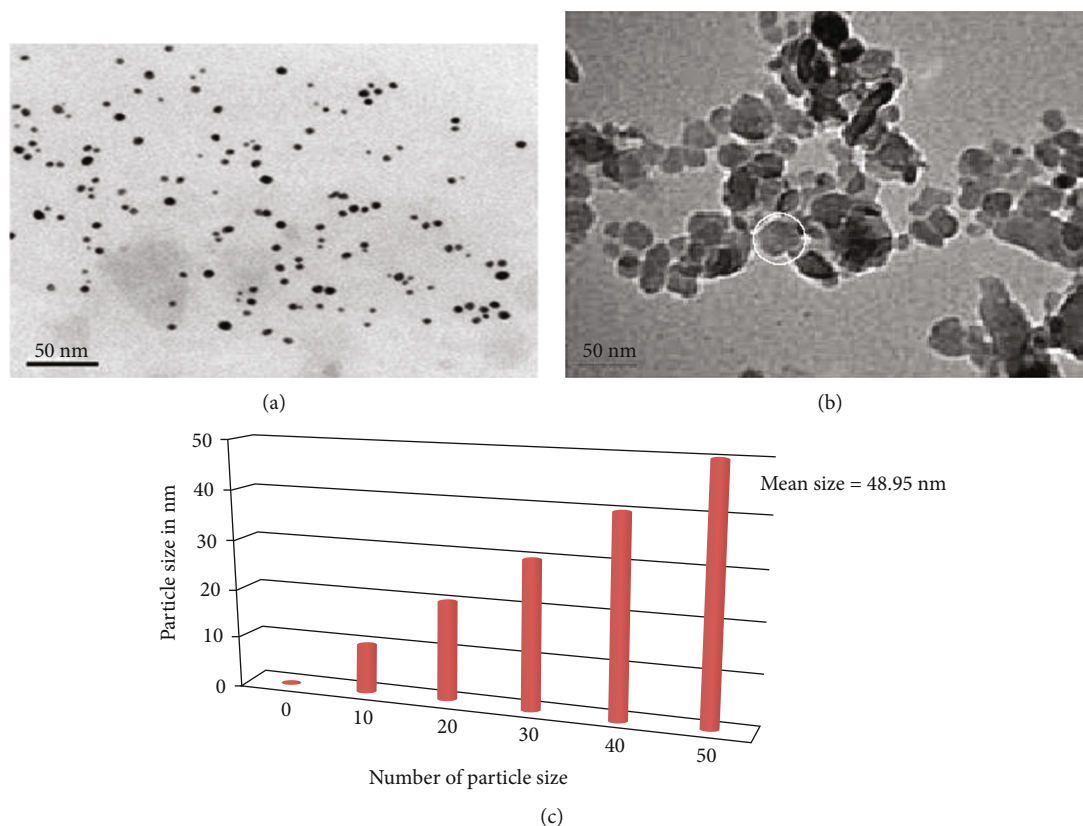
(a)

(b)

Mean size = 48.95 nm

(c)

FIGURE 3: TEM image of pure (a) ZnO, (b) ZnO NPs, and (c) particle size distribution.

ammonia solution before being washed with ethanol multiple times. The precipitates were then vacuum dried for 13 hours before being calcined in a hot air oven at 350°C for 4.5 hours (Figure 2). The presence of white powder in the response combination is a clear evidence of the formation of ZnO NPs. The zinc oxide nanoparticles were then collected and stored in vacuum for future use.

(1) Synthesis of (2,4,5,6)-2-(((2-Aminoethyl)Amino)Methyl)-5-((4-Fluroro Benzylidene)Amino-3,6-Dimethoxytetrahydro-2H-Pyran-4-ol (1a). These are as follows: IR (kBr) (cm^{-1}); 3674 (NH, str), 3278 (OH-str), 2987 (CH-str Ar ring), 2900 (CH, str), 1645 (N=CH, str), 1405 (NH$_2$, bending), 1393 (N-C, str); ^{1}H NMR (DMSO-d$_6$), δ (ppm): 8.77 (s, 1H, N=CH), 7.46–7.81 (m, 4H, F-Ph), 5.15 (s, 2H, NH$_2$), 5.16-3.05 (m, 5H, CS-H), 3.55 (s, 1H, CS-OH), 3.48-3.35 (s, 6H, OCH$_3$-CS), 2.82-2.56 (m, 2H, CH$_2$-NH), 2.78-2.61 (m, 4H, N (CH$_2$)$_2$), 2.0 (s, 1H, NH); and ^{13}C NMR (DMSO-d$_6$) δ (ppm): 165.4, 130.8, 115.9, 115.8 (6C, F-Ph), 163.8 (1C, N=CH), 114.3, 93.4, 73.5, 65.4, 36.7 (5C, CS), 70.4 (1C, N-CH), 57.9, 55.8 (2C, OCH$_3$-CS), 51.2, 41.4 (2C, N-C in amine).

(2) Synthesis of (2,4,5,6)-2-(((2-Aminoethyl)Amino)Methyl)-5-((4-Chlorbenzylidene)Amino-3,6-Dimethoxytetrahydro-2H-Pyran-4-ol (1b). These are as follows: IR (kBr) (cm^{-1}); 3672 (NH, str), 3280 (OH-str), 2989 (CH-str Ar ring), 2902 (CH, str), 1640 (N=CH, str), 1407 (NH$_2$, bending), 491 (C-Cl); ^{1}H NMR (DMSO-d$_6$), δ (ppm): 8.76 (s, 1H, N=CH) 7.96–7.51
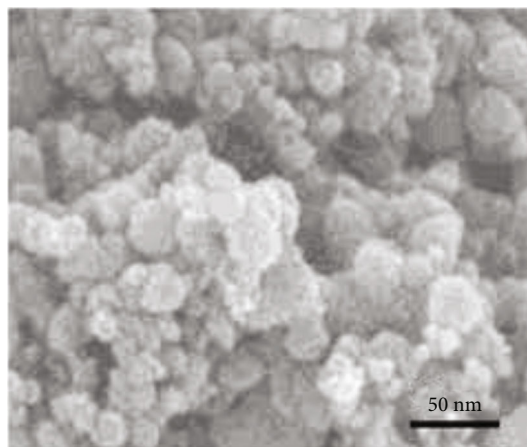
FIGURE 4: SEM image of ZnO nanoparticles.

(m, 4H, Cl-Ph), 5.16 (s, 2H, NH$_2$), 4.17-3.67 (m, 5H, CS-H), 3.55 (s, 1H, CS-OH), 3.45-3.32 (s, 6H, OCH$_3$-CS), 2.85-2.58 (m, 2H, CH$_2$-NH), 2.76 (m, 4H, N (CH$_2$)$_2$), 2.07 (s, 1H, NH); and ^{13}C NMR (DMSO-d$_6$) δ (ppm): 163.5 (1C, N=CH), 135.4, 125.3, 120.4, 116.5 (6C, Cl-Ph), 114.0, 93.2, 73.3, 65.6, 36.9 (5C, CS), 71.5 (1C, N-CH), 57.6, 55.4 (2C, OCH$_3$-CS), 51.0, 41.3 (2C, N-C in amine).

(3) Synthesis of (2,4,5,6)-2-(((2-Aminoethyl)Amino)Methyl)-5-((4-Hydroxybenzylidene)Amino-3,6-Dimethoxytetrahydro-2H-Pyran-4-ol (1c). These are as follows: IR (kBr) (cm^{-1});

Figure 5: X-ray diffraction study of (a) pure chitosan and (b) chitosan derivative.

3676 (NH, str), 3286 (OH-str), 2991 (CH-str Ar ring), 2904 (CH, str), 1644 (N=CH, str), 1408 (NH$_2$, bending), 1395 (N-C, str); ^{1}H NMR (DMSO-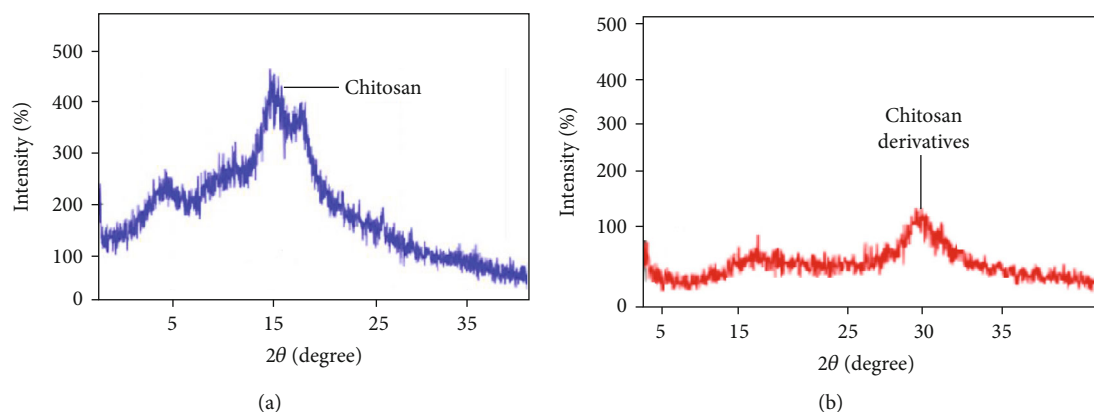d$_6$), δ (ppm): 10.62 (s, 1H, Ph-OH), 8.70 (s, 1H, N=CH), 7.87,(m, 4H, OH-Ph), 5.12 (s, 2H, NH$_2$), 4.20-3.63 (m, 5H, CS-H), 3.56 (s, 1H, CS-OH), 3.47-3.33 (s, 6H, OCH$_3$-CS), 2.80-2.55 (m, 2H, CH$_2$-NH), 2.74-2.65 (m, 4H, N(CH$_2$)$_2$), 2.05 (s, 1H, NH); and ^{13}C NMR (DMSO-d$_6$) δ (ppm): 163.3 (1C, N=CH), 161.7, 129.5, 120.2, 116.5 (6C, OH-Ph), 112.1, 92.0, 72.2, 64.6, 37.9 (5C, CS), 71.0 (1C, N-CH), 57.8, 55.6 (2C, OCH$_3$-CS), 51.3, 41.2 (2C, N-C in amine).
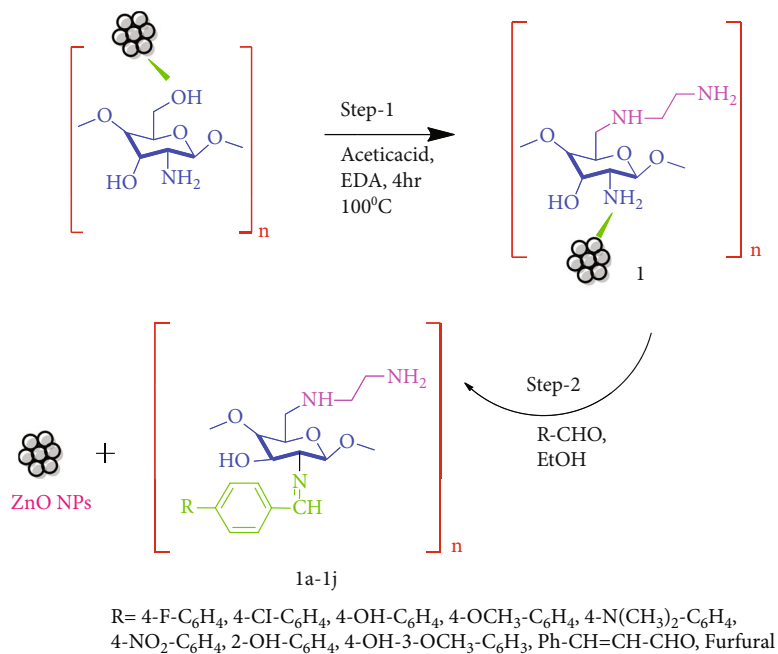
(4) Synthesis of (2,4,5,6)-2-(((2-Aminoethyl)Amino)Methyl)-5-((4-Methoxybenzylidene)Amino-3,6-Dimethoxytetrahydro-2H-Pyran-4-ol (1d). These are as follows: IR (kBr) (cm^{-1}); 3679 (NH, str), 3280 (OH-str), 2981 (CH-str Ar ring), 2906 (CH, str), 1631 (N=CH, str), 1404 (NH$_2$, bending), 1391 (N-C, str); ^{1}H NMR(DMSO-d$_6$), δ (ppm): 8.79 (s, 1H, N=CH) 8.13-7.72 (m, 4H, OCH$_3$-Ph), 5.17 (s, 2H, NH$_2$), 4.17-3.66 (m, 5H, CS-H), 3.87 (s, 3H, OCH$_3$), 3.58 (s, 1H, CS-OH), 3.52-3.36 (s, 6H, OCH$_3$-CS), 2.84-2.57 (m, 2H, CH$_2$-NH), 2.70-2.63 (m, 4H, N(CH$_2$)$_2$), 2.05 (s, 1H, NH); and ^{13}C NMR (DMSO-d$_6$) δ (ppm): 163.9 (1C, N=CH), 160.6, 130.2, 124.3, 114.5 (6C, OCH$_3$-Ph), 112.4, 92.3, 72.4, 64.3, 37.5 (5C, CS), 71.5 (1C, N-CH), 57.4, 55.7 (2C, OCH$_3$-CS), 55.3 (1C, OCH$_3$-Ph), 51.3, 41.2 (2C, N-C in amine).

(5) Synthesis of (2,4,5,6)-2-(((2-Aminoethyl)Amino)Methyl)-5-((4-Dimethylamino)Bezylidene)Amino)-3,6-Dimethoxyte-trahydro-2H-Pyran-4-ol (1e). These are as follows: IR (kBr) (cm^{-1}); 3677 (NH, str), 3285 (OH-str), 2988 (CH-str Ar ring), 2910 (CH, str), 1642 (N=CH, str), 1404 (NH$_2$, bending), 1392 (N-C, str); ^{1}H NMR(DMSO-d$_6$), δ (ppm): 8.72 (s, 1H, N=CH), 7.58-6.75 (m, 4H, N(CH$_3$)$_2$-Ph), 5.10 (s, 2H, NH$_2$), 4.19-3.69 (m, 5H, CS-H), 3.58 (s, 1H, CS-OH), 3.50-3.31 (s, 6H,OCH$_3$-CS), 3.02 (s, 6H, N(CH$_3$)$_2$), 2.80-2.50 (m, 2H, CH$_2$-NH), 2.73-2.65 (m, 4H, N(CH$_2$)$_2$), 2.07 (s, 1H, NH); and ^{13}C NMR (DMSO-d$_6$) δ (ppm): 163.7 (1C, N=CH), 152.6, 129.9, 122.8, 113.6, 21.4 (8C, N(CH$_3$)$_2$-Ph), 112.6, 92.5, 72.7, 64.6, 37.8 (5C, CS), 71.8 (1C, N-CH), 57.8, 55.7 (2C, OCH$_3$-CS), 51.3, 41.0 (2C, N-C in amine).

(6) Synthesis of (2,4,5,6)-2-(((2-Aminoethyl)Amino)Methyl)-3,6-Dimethoxy-5-((4-Nitrobenzylidene)Amino)Tetrahydro-2H-Pyran-4-ol (1f). These are as follows: IR (kBr) (cm^{-1}); 3670 (NH, str), 3276 (OH-str), 2978 (CH-str Ar ring), 2908 (CH, str), 1634 (N=CH, str), 1546 (N-O, str), 1408 (NH$_2$, bending), 1395 (N-C, str); ^{1}H NMR(DMSO-d$_6$), δ (ppm): 8.73 (s, 1H, N=CH), 8.51–8.32 (m, 4H, NO$_2$-Ph), 5.19 (s, 2H, NH$_2$), 4.20-3.60 (m, 5H, CS-H), 3.58 (s, 1H, CS-OH), 3.55-3.34 (s, 6H, OCH$_3$-CS), 2.88-2.58 (m, 2H, CH$_2$-NH), 2.77-2.63 (m, 4H, N(CH$_2$)$_2$), 2.09 (s, 1H, NH); and ^{13}C NMR (DMSO-d$_6$) δ (ppm): 164.5 (1C, N=CH), 148.3, 136.1, 135.3, 130.1, 129.5, 123.6 (6C, NO$_2$-Ph), 112.1, 92.2, 72.3, 64.4, 37.5 (5C, CS), 91.8 (1C, N-CH), 57.8, 55.3 (2C, OCH$_3$-CS), 51.3, 41.4 (2C, N-C in amine).

(7) Synthesis of 2,4,5,6)-2-(((2-Aminoethyl)Amino)Methyl)-5-((2-Hydroxybenzylidene) Amino)-3,6-Dimethoxytetrahy-dro-2H-Pyran-4-ol (1g). These are as follows: IR (kBr) (cm^{-1}); 3672 (NH, str), 3284 (OH-str), 2982 (CH-str Ar ring), 2911 (CH, str), 1648 (N=CH, str), 1403 (NH$_2$ bending), 1392 (N-C, str); ^{1}H NMR (DMSO-d$_6$), δ (ppm): 8.78 (s, 1H, N=CH) 7.82–7.11 (m, 4H, OH-Ph), 5.46 (s, 1H, OH-Ph), 5.16 (s, 2H, NH$_2$), 4.22-3.69 (m, 5H, CS-H), 3.52 (s, 1H, CS-OH), 3.52-3.32 (s, 6H, OCH$_3$-CS), 2.83-2.53 (m, 2H, CH$_2$-NH), 2.78-2.64 (m, 4H, N(CH$_2$)$_2$), 2.05 (s, 1H, NH); and ^{13}C NMR (DMSO-d$_6$) δ (ppm): 163.5 (1C, N=CH), 162.7, 136.5, 132.8, 124.5, 123.4, 120.4 (6C, OH-Ph), 112.0, 92.1, 72.2, 64.3, 37.4 (5C, CS), 91.2 (1C,N-CH), 57.8, 55.5 (2C, OCH3-CS), 51.5, 42.5 (2C, N-C in amine).

(8) Synthesis of (2,4,5,6)-2-(((2-Aminoethyl)Amino)Methyl)-5-((4-Hydroxy-3-Methoxybenzyline)Amino)-3,6-Dimethoxy-tetrahydro-2H-Pyran-4-ol (1h). These are as follows: IR (kBr) (cm^{-1}); 3670 (NH, str), 3275 (OH-str), 2980 (CH-str Ar ring), 2903 (CH, str), 1635 (N=CH, str), 1406 (NH$_2$, bending), 1390 (N-C, str); ^{1}H NMR (DMSO-d$_6$), δ (ppm): 8.69 (s, 1H, N=CH), 7.42–6.75 (m, 3H, vanillin), 5.35 (s, 1H, OH-Ph), 5.25 (s, 2H, NH$_2$), 4.26-3.66 (m, 5H, CS-H), 3.74 (s, 3H, OCH$_3$), 3.59 (s, 1H, CS-OH), 3.53-3.31 (s, 6H, OCH$_3$-CS), 2.86-2.58 (m, 2H, CH$_2$-NH), 2.79-2.67 (m, 4H, N(CH$_2$)$_2$), 2.09 (s, 1H, NH); and ^{13}C NMR (DMSO-d$_6$) δ (ppm): 163.2 (1C, N=CH), 154.5, 149.6, 130.4, 125.2, 117.4, 110.5 (6C, vanillin), 112.3, 92.8, 72.6, 64.5, 37.7 (5C, CS),

R= 4-F-C_6H_4, 4-CI-C_6H_4, 4-OH-C_6H_4, 4-OCH$_3$-C_6H_4, 4-N(CH$_3$)$_2$-C_6H_4, 4-NO$_2$-C_6H_4, 2-OH-C_6H_4, 4-OH-3-OCH$_3$-C_6H_3, Ph-CH=CH-CHO, Furfural

SCHEME 1: Synthesis of chitosan derivatives 1a-1j using ZnO NPs as a catalyst.
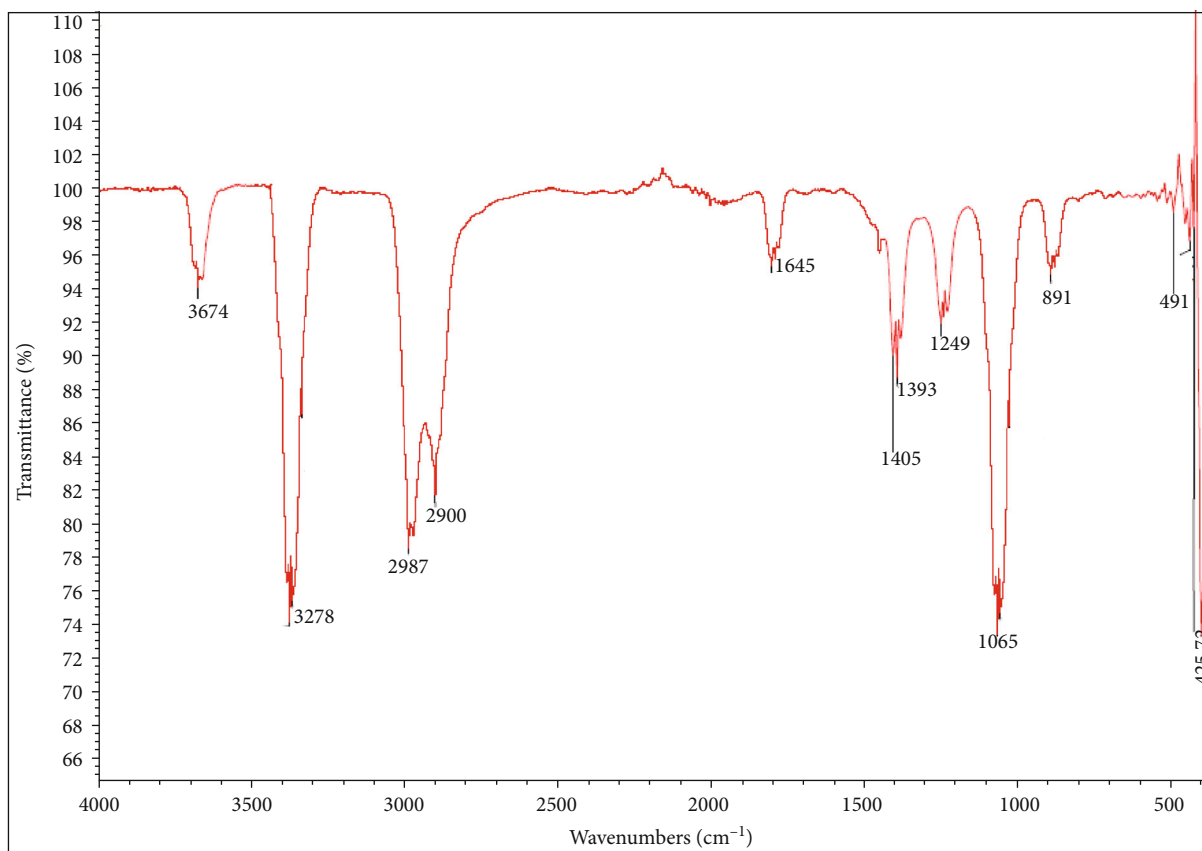
FIGURE 6: FTIR spectrum of compound 1a.

Compound-1b is highly active
in gram negative *E. coli*
$a = 4.0\,\mu g/mL$, *E. coli*, $b = 32\,\mu g/mL$
$c = $ DMSO, $d = $ standard

Compound-1h is highly active
in gram positive *S. aureus*
$a = 6.0\,\mu g/mL$, *S. aureus*, $b = 32\,\mu g/mL$
$c = $ DMSO, $d = $ standard
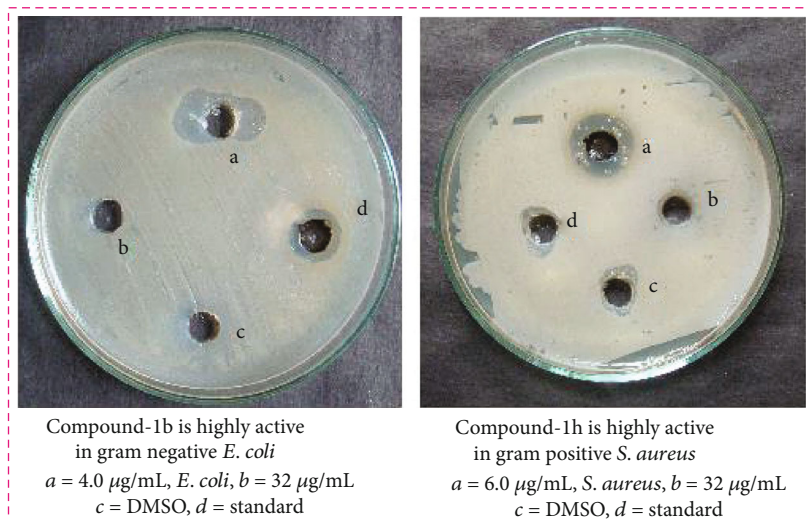
FIGURE 7: Antibacterial assay of highly active compounds with erythromycin.

91.3 (1C,N-CH), 57.5 (1C, OCH$_3$), 57.0, 55.2 (2C, OCH3-CS), 51.7, 42.5 (2C, N-C in amine).

(9) Synthesis of (2,4,5,6)-2-(((2-Aminoethyl)Amino)Methyl)-3,6-Dimethoxy-5-((3-Phenylallylidene)Amino)Tetrahydro-2H-Pyran-4-ol (1i). IR (kBr) (cm^{-1}); 3682 (NH, str), 3281 (OH-str), 2982 (CH-str Ar ring), 2907 (CH, str), 1643 (N=CH, str), 1410 (NH$_2$ bending), 1391 (N-C-, str); ^{1}H NMR (DMSO-d$_6$), δ (ppm): 8.77 (s, 1H, N=CH), 7.62, 7.41, 7.35 (m, 5H, Ph), 7.05, 6.44 (d, 2H, CH=CH, $J = 7.0$) 5.19 (s, 2H, NH$_2$), 4.18-3.69 (m, 5H, CS-H), 3.59-3.34 (s, 6H, OCH$_3$-CS), 3.38 (s, 1H, CS-OH), 2.88-2.59 (s, 2H, CH$_2$-NH), 2.71 (m, 4H, N(CH$_2$)$_2$), 2.01 (s, 1H, NH); and ^{13}C NMR (DMSO-d$_6$) δ (ppm): 163.6 (1C, N=CH), 135.2, 128.9, 128.6, 127.9 (6C, Ph), 131.5 (2C,C=C, Ph), 113.2, 92.4, 72.2, 64.1, 37.3 (5C, CS), 91.6 (1C, N-CH), 57.4, 55.8 (2C, OCH$_3$-CS), 51.3, 42.5 (2C, N-C in amine).

(10) Synthesis of (2,4,5,6)-2-(((2-Aminoethyl)Amino)-Methyl)-5-((Furan-2-yl-Methylene)Amino)-3,6-Dimethoxyte-trahydro-2H-Pyran-4-ol (1j). IR (kBr) (cm^{-1}); 3686 (NH, str), 3284 (OH-str), 2983 (CH-str Ar ring), 2902 (CH, str), 1637 (N=CH, str), 1406 (NH$_2$, bending), 1398 (N-C, str); ^{1}H NMR (DMSO-d$_6$), δ (ppm): 8.76 (s, 1H, N=CH), 7.75-6.96 (m, 3H, furfural), 5.16 (s, 2H, NH$_2$), 4.18-3.66 (m, 5H, CS-H), 3.52-3.36 (s, 6H, OCH$_3$-CS), 3.33 (s, 1H, CS-OH), 2.85-2.55 (s, 2H, CH$_2$-NH), 2.75-2.62 (m, 4H, N(CH$_2$)$_2$), 2.03 (s, 1H, NH); and ^{13}C NMR (DMSO-d$_6$) δ (ppm): 163.7 (1C, N=CH), 155.3, 148.2, 123.5, 114.8 (4C, furfural), 112.7, 92.6, 72.5, 64.4, 37.8 (5C, CS), 91.7 (1C,N-CH), 57.5, 55.1 (2C, OCH$_3$-CS), 51.8, 42.9 (2C, N-C in amine).

2.3. In Vitro Antimicrobial Screening. Using a previously reported approach [60], the antibacterial activity of the compounds 1a-1j was evaluated against the bacterial strains *Staphylococcus aureus* (ATCC-25923), *Streptococcus pneumoniae, Escherichia coli* (ATCC-25922), and *Pseudomonas aeruginosa* (ATCC-27853). The minimal inhibitory concentration for each of the produced substances was determined.

TABLE 1: Antibacterial activity of gram negative and gram positive for compounds 1a-1j with their MIC values.

Compounds no	Gram negative (μg/mL)		Gram positive (μg/mL)	
	E. coli	P. aeruginosa	S. pneumonia	S. aureus
1a	6	30	5	14
1b	4	6	32	15
1c	8	12	6	13
1d	34	18	9	10
1e	10	20	12	30
1f	16	7	6	15
1g	20	8	16	12
1h	18	9	13	6
1i	9	10	26	14
1j	11	16	18	9
Erythromycin	6	6	4	8

The test samples were dissolved in DMSO (dimethylsulfoxide) at a concentration of 64 μg/mL for each sample. Various dilutions (64, 32, and 0.5 μg/mL) were made using twofold dilutions. The microbe suspensions containing 106 CFU/mL were injected into the matched wells and incubated at 36°C for 24 hours.

3. Results and Discussion

3.1. Characterization of Zinc Oxide Nanoparticles

3.1.1. Transmission Electron Microscopy (TEM). The size and morphology of the ZnO nanoparticles were determined using a TEM examination. Figure 3 shows a TEM image of both pure ZnO and ZnO NPs. In the range of 50 nm, the TEM image clearly shows the spherical shape of the ZnO NPs.

3.1.2. Scanning Electron Microscopy (SEM). SEM analysis revealed well-defined, uniformly spherical ZnO NPs with
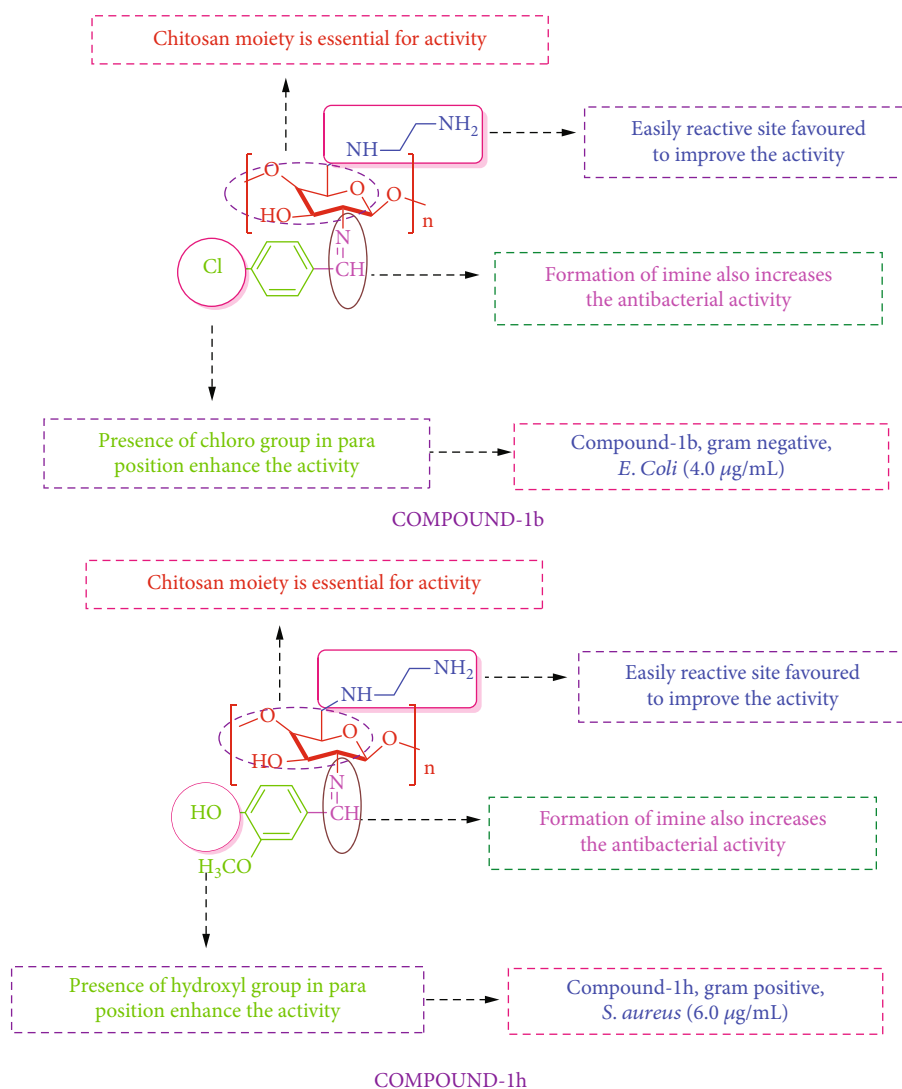
Figure 8: SAR relationship of highly active compounds.

no aggregation and a very small size. *Mentha pipertia* has a lot of charged surfaces that are great for binding metal ions from their watery precursor solution. Figure 4 displays a scanning electron microscope image of zinc oxide nanoparticles. The SEM picture revealed a nanoparticle with a diameter of 50 nm and a roughly spherical shape.

3.1.3. XRD (or) X-Ray Diffraction Study.

An X-ray diffraction investigation was carried out on chitosan and chitosan derivatives. Figure 5 [61] shows chitosan with very wide peaks at $2\theta = 15°$ and $2\theta = 30°$. The chitosan derivatives displayed two faint peaks at 2θ of $15°$ and $30°$ in Figure 5. The peaks establish for chitosan at $2\theta = 15°$ vanished in chitosan derivatives while the very broad peaks at $30°$ became weak, showing that chitosan has moral compatibility and good formation of porous xerogel network. According to the XRD results, the chitosan derivatives are amourphous in nature.

3.1.4. Recovery of Catalyst.

Catalyst recovery is important in the biosynthetic process. We tested their recyclability twice with essentially equal catalytic activity using the Schiff base of chitosan derivative (1a-1j) zinc oxide nanoparticle reaction. Following the addition of DMF, the ZnO NPs were centrifuged and washed with EtOH to remove any residual product.

3.2. Chemistry

3.2.1. Preparation of Chitosan Analogue (1, 1a–1j).

Chitosan (2 g, deactylated) was dissolved in 20 ml of 1% acetic acid solution (pH = 3.6 – 3.7), and ethylenediamine (0.7 mL) was reacted at 100°C for 4 hrs using ZnO NPs as a green catalyst to get compound 1. After adding 1 M NaOH for adjusting the (pH = 4.0) of compound 1. A compound 1 (2.5 g dissolved in acetic acid with ethanol) and 4-flurobenzaldehyde (1.2 g) in ethanol stirring for 8 hrs at 60°C with ZnO NPs used as a catalyst. The obtained white gel indicates the formation of compound 1a. The resulting product was precipitated in a solution of 5% sodium hydroxide. The precipitate was filtered and washed with ice-cold

water and ethanol to remove the unreactants of aldehyde and ketone. The final product was soluble in DMF. TLC was used to track the reaction's progress. In TLC, the eluting solvents were hexane and ethyl acetate (4:6). Compounds 1b–1j were synthesized using the technique described above.

The novel chitosan compounds were established by analytical technique, such as FT-IR, ^{1}H NMR, and ^{13}C NMR as seen in Supplementary Materials (available here). The FT-IR spectra exhibited absorption bands (1a–1j) at 3674, 3278, 2987, 2900, 1645, 1405, and 1393 cm^{-1}, confirming NH, OH, Ar-H, CH, N=CH, NH_2, and N-C groups. The ^{1}H NMR spectra (1a–1j) indicate chemical shift values at 10.60, 8.79–8.69, 8.13–7.46, 5.16–5.10, 3.58-3.52, 3.45, and 2.82 ppm, confirming OH, N=CH, Ph-CH, NH_2,CS-OH, OCH_3 and CH_2-NH protons, respectively. The ^{13}C NMR showed (1b–1j) signals at 164.5–163.3, 91.2–71.0, 57.9-55.4, and 51.3-41.0 ppm, confirming the N=CH, N-CH, OCH_3, and N-C of carbon atoms. Scheme 1 illustrates the synthesis of chitosan derivatives.

3.2.2. Fourier Transform Infrared (FTIR) Spectroscopy. In FTIR spectra of chitosan, NH peak was observed at 3674 cm^{-1} which can be assigned to stretching vibration of amino group, and another peak observed at 3278 cm^{-1} can be attributed to hydroxyl group (O-H, str). Similarly, the stretching vibration of carbon and hydrogen in aromatic ring was observed at 2987 cm^{-1}. The weak band at 2900 cm^{-1} can be assigned to symmetric stretching of carbon–hydrogen (C-H, str), and a sharp characteristic peak at 1645 cm^{-1} can be attributed to stretching vibration of imine linkage (N=CH, str). In the chitosan-Schiff base, the bending vibration of amide observed at 1405 cm^{-1} can be assigned to (NH_2, bending), and another sharp peak at 1393 cm^{-1} can be attributed to stretching vibration of (N-C, str). The FTIR spectrum of compound 1a is present in Figure 6.

3.3. In Vitro Antibacterial Activity Analysis. The antibacterial activity of chitosan derivatives of 1a-1j was tested *in vitro* against *S. aureus* (ATCC-25923), *S. pneumoniae, E. coli* (ATCC-25922), and *P. aeruginosa* (ATCC-27853). As a control, erythromycin was utilized. Compound 1b (4.0 μg/ mL, *E. coli*) is highly active, and compound 1h (6.0 μg/mL, *S. aureus*) is highly active compared with the standard drug. The antibacterial assay images are present in Figure 7, and MIC values are shown in Table 1.

3.4. Structure Activity Relationship. The structure activity relationship is a relationship that exists between a molecule chemical structure and its antibacterial activity. SAR analysis allows for the identification of chemical groups responsible for inducing antibacterial activity in the organism. The SAR was evaluated using the antibacterial activity of chitosan derivatives. The compounds 1b and 1h are highly active compared with control erythromycin and other compounds. Because of the reason due to the presence of chloro (Cl) and hydroxyl (-OH) groups at para position in phenyl moiety, it was exhibited to be highly active against 1b (4.0 μg/mL, *E. coli*, gram −ve) and 1h (6.0 μg/mL, *S. aureus*, gram +ve) bac-

teria when compared to standard erythromycin. Figure 8 demonstrates the SAR of highly active compounds.

4. Conclusions

Chitosan possesses different functional groups (i.e., hydroxyl and amine groups) that help to prepare new chitosan derivatives. The present study intends to develop newly synthesized Schiff base of chitosan polymer derivatives 1a-1j so we are focused the green synthetic method for the synthesis of zinc oxide nanoparticles (ZnO NPs) using extract of Mentha piperita, which can reduce zinc oxide ions into ZnO NPs in a simple way. The newly formed Schiff bases 1a-1j were synthesized using ZnO NPs as a catalyst and were confirmed by FTIR, NMR, TEM, SEM, and XRD. Moreover, the antibacterial activity revealed that compound 1b (4.0 μg/ mL, E. coli) is highly active against gram-negative bacteria, and compound 1h (6.0 μg/mL, S. aureus) is moderate active against gram-positive bacteria. In future, compounds 1b and 1h can be developed as an antibacterial drug.

Data Availability

The supplementary file data used to support the findings of this study are included within the supplementary information files.

Conflicts of Interest

The authors declare no conflict of interest.

Authors' Contributions

Ponnusamy Packialakshmi and Perumal Gobinath both are equally contributed.

Acknowledgments

Supplementary Materials

The supplementary file contains ^{1}H NMR and ^{13}C NMR spectra. *(Supplementary Materials)*

References

[1] M. M. G. Fouda, M. R. El-Aassar, and S. S. Al-Deyab, "Antimicrobial activity of carboxymethyl chitosan/polyethylene oxide nanofibers embedded silver nanoparticles," *Carbohydrate Polymers*, vol. 92, no. 2, pp. 1012–1017, 2013.

[2] R. M. Abdel-Rahman, A. M. Abdel-Mohsen, M. M. G. Fouda, S. S. Al Deyab, and A. S. Mohamed, "Finishing of cellulosic fabrics with chitosan/polyethylene glycol-siloxane to improve their performance and antibacterial properties," *Life Science Journal*, vol. 10, pp. 834–839, 2013.

[3] G. S. Dhillon, S. Kaur, S. K. Brar, and M. Verma, "Green synthesis approach: extraction of chitosan from fungus mycelia,"

Critical Reviews in Biotechnology, vol. 33, no. 4, pp. 379–403, 2013.

[4] E. Ibitoye, I. Lokman, M. Hezmee, Y. Goh, A. Zuki, and A. Jimoh, "Extraction and physicochemical characterization of chitin and chitosan isolated from house cricket," *Biomedical Materials*, vol. 13, no. 2, article 025009, 2018.

[5] C. Y. Soon, Y. B. Tee, C. H. Tan, A. T. Rosnita, and A. Khalina, "Extraction and physicochemical characterization of chitin and chitosan from _Zophobas morio_ larvae in varying sodium hydroxide concentration," *International Journal of Biological Macromolecules*, vol. 108, pp. 135–142, 2018.

[6] M. Hamdine, M. C. Heuzey, and A. Begin, "Effect of organic and inorganic acids on concentrated chitosan solutions and gels," *International Journal of Biological Macromolecules*, vol. 37, no. 3, pp. 134–142, 2005.

[7] M. Kong, X. G. Chen, K. Xing, and H. J. Park, "Antimicrobial properties of chitosan and mode of action: a state of the art review," *International Journal of Food Microbiology*, vol. 144, no. 1, pp. 51–63, 2010.

[8] H. Barabadi, A. Mohammadzadeh, H. Vahidi et al., "Penicillium chrysogenum-derived silver nanoparticles: exploration of their antibacterial and biofilm inhibitory activity against the standard and pathogenic Acinetobacter baumannii compared to tetracycline," *Journal of Cluster Science*, 2021.

[9] G. Madhan, A. A. Begam, L. V. Varsha, R. Ranjithkumar, and D. Bharathi, "Facile synthesis and characterization of chitosan/zinc oxide nanocomposite for enhanced antibacterial and photocatalytic activity," *International Journal of Biological Macromolecules*, vol. 190, pp. 259–269, 2021.

[10] R. C. Goy, D. de Britto, and O. B. G. Assis, "A review of the antimicrobial activity of chitosan," *Polímeros: Ciencia e Tecnologia*, vol. 19, no. 3, pp. 241–247, 2009.

[11] A. M. Omer, T. M. Tamer, M. A. Hassan, P. Rychter, M. S. MohyEldin, and N. Koseva, "Development of amphoteric alginate/aminated chitosan coated microbeads for oral protein delivery," *International Journal of Biological Macromolecules*, vol. 92, pp. 362–370, 2016.

[12] M. Y. Aksoy and B. H. Beck, "Antimicrobial activity of chitosan and a chitosan oligomer against bacterial pathogens of warmwater fish," *Journal of Applied Microbiology*, vol. 122, no. 6, pp. 1570–1578, 2017.

[13] K. Valachova, T. M. Tamer, M. M. Eldin, and L. Soltes, "Radical-scavenging activity of glutathione, chitin derivatives and their combination," *Chemical Papers*, vol. 70, no. 6, pp. 820–827, 2016.

[14] F. Xie, R. L. Ding, W. F. He et al., "In vivo antitumor effect of endostatin-loaded chitosan nanoparticles combined with paclitaxel on Lewis lung carcinoma," *Drug Delivery*, vol. 24, no. 1, pp. 1410–1418, 2017.

[15] D. Archana, J. Dutta, and P. K. Dutta, "Evaluation of chitosan nano dressing for wound healing: characterization, in vitro and in vivo studies," *International Journal of Biological Macromolecules*, vol. 57, pp. 193–203, 2013.

[16] T. M. Tamer, M. Collins, K. Valachová et al., "MitoQ loaded chitosan-hyaluronan composite membranes for wound healing," *Materials*, vol. 11, no. 4, p. 569, 2018.

[17] F. L. Mi, Y. C. Tan, H. F. Liang, and H. W. Sung, "In vivo biocompatibility and degradability of a novel injectable-chitosan-based implant," *Biomaterials*, vol. 23, no. 1, pp. 181–191, 2002.

[18] T. M. Tamer, K. Valachova, M. A. Hassan et al., "Chitosan/hyaluronan/edaravone membranes for anti-inflammatory wound dressing: _In vitro_ and _in vivo_ evaluation studies," *Materials Science and Engineering*, vol. 90, pp. 227–235, 2018.

[19] A. Khatua, A. Prasad, E. Priyadarshini et al., "Emerging antineoplastic plant-based gold nanoparticle synthesis: a mechanistic exploration of their anticancer activity toward cervical cancer cells," *Journal of Cluster Science*, vol. 31, pp. 1329–1340, 2019.

[20] H. Barabadi, H. Vahidi, K. D. Kamali et al., "Emerging theranostic gold nanomaterials to combat lung cancer: a systematic review," *Journal of Cluster Science*, vol. 31, pp. 323–330, 2020.

[21] H. Barabadi, H. Vahidi, M. A. Mahjoub et al., "Emerging antineoplastic gold nanomaterials for cervical cancer therapeutics: a systematic review," *Journal of Cluster Science*, vol. 31, pp. 1173–1184, 2020.

[22] H. Barabadi, H. Vahidi, K. D. Kamali, M. Rashedi, and M. Saravanan, "Antineoplastic biogenic silver nanomaterials to combat cervical cancer: a novel approach in cancer therapeutics," *Journal of Cluster Science*, vol. 31, no. 4, pp. 659–672, 2020.

[23] M. Saravanan, H. Barabadi, B. Ramachandran, G. Venkatraman, and K. Ponmurugan, "Emerging plant-based anti-cancer green nanomaterials in present scenario," *Comprehensive Analytical Chemistry*, vol. 87, pp. 291–318, 2019.

[24] H. Barabadi, F. Mojab, H. Vahidi et al., "Green synthesis, characterization, antibacterial and biofilm inhibitory activity of silver nanoparticles compared to commercial silver nanoparticles," *Inorganic Chemistry Communications*, vol. 129, article 108647, 2021.

[25] N. Strbo, N. Yin, and O. Stojadinovic, "Innate and adaptive immune responses in wound epithelialization," *Advances in Wound Care*, vol. 3, no. 7, pp. 492–501, 2014.

[26] O. Takeuchi and S. Akira, "Pattern recognition receptors and inflammation," *Cell*, vol. 140, no. 6, pp. 805–820, 2010.

[27] M. Christopher, J. H. Thomas, L. Christine, J. Willis, and T. Simpson, "Resistance to and synthesis of the antibiotic mupirocin," *Nature reviews Microbiology*, vol. 8, no. 4, pp. 281–289, 2010.

[28] N. Bala, S. Saha, M. Chakraborty et al., "Green synthesis of zinc oxide nanoparticles using Hibiscus subdariffa leaf extract: effect of temperature on synthesis, anti-bacterial activity and anti-diabetic activity," *RSC Advances*, vol. 5, no. 7, pp. 4993–5003, 2015.

[29] W. J. Rasmussen, E. Martinez, P. Louka, and G. D. Wingett, "Zinc oxide nanoparticles for selective destruction of tumor cells and potential for drug delivery applications," *Expert opinion on drug delivery*, vol. 7, no. 9, pp. 1063–1077, 2010.

[30] H. S. Yoon and J. D. Kim, "Fabrication and characterization of ZnO films for biological sensor application of FPW device," *Applications of ferroelectrics 15th IEEE international symposium*, vol. 3, pp. 322–325, 2006.

[31] M. H. Xiong, "ZnO nanoparticles applied to bioimaging and drug delivery," *Advanced Materials*, vol. 25, no. 37, pp. 5329–5335, 2013.

[32] L. Nie, L. Gao, P. Feng et al., "Three-dimensional functionalized tetrapod like ZnO nanostructures for plasmid DNA delivery," *Small*, vol. 2, no. 5, pp. 621–625, 2006.

[33] G. Applerot, A. Lipovsky, R. Dror, and N. Perkas, "Enhanced antibacterial activity of Nanocrystalline ZnO due to increased ROS-mediated cell injury," *Advanced Functional Materials*, vol. 19, no. 6, pp. 842–852, 2009.

[34] S. Nair, "Role of size scale of ZnO nanoparticles and microparticles on toxicity toward bacteria and osteoblast cancer cells," *Journal of Materials Science: Materials in Medicine*, vol. 20, no. S1, pp. 235–241, 2009.

[35] V. A. Kirthi, A. A. Rahuman, G. Rajakumar, and S. Marimuthu, "Acaricidal, pediculocidal and larvicidal activity of synthesized ZnO nanoparticles using wet chemical route against blood feeding parasites," *Parasitology research*, vol. 109, no. 2, pp. 461–472, 2011.

[36] A. Alkaladi, M. A. Abdelazim, and M. Afifi, "Antidiabetic activity of zinc oxide and silver nanoparticles on streptozotocin-induced diabetic rats," *International Journal of Molecular Sciences*, vol. 15, no. 2, pp. 2015–2023, 2014.

[37] H. Yilmaz Atay, *Antibacterial activity of chitosan-based systems*, Springer nature, 2019.

[38] P. A. Felse and T. Panda, "Studies on applications of chitin and its derivatives," *bioprocess and biosystems engineering*, vol. 20, no. 6, pp. 505–512, 1999.

[39] C. M. Lehr, J. A. Bouwstra, E. H. Schacht, and H. E. Junginger, "In vitro evaluation of mucoadhesive properties of chitosan and some other natural polymers," *International Journal of Pharmaceutics*, vol. 78, no. 1-3, pp. 43–48, 1992.

[40] N. M. Alvesa and J. F. Mano, "Chitosan derivatives obtained by chemical modifications for biomedical and environmental applications," *International Journal of Biological Macromolecules*, vol. 43, no. 5, pp. 401–414, 2008.

[41] E. B. Mirzaei, A. S. A. Ramazani, M. Shafiee, and M. Danaei, "Studies on Glutaraldehyde Crosslinked Chitosan Hydrogel Properties for Drug Delivery Systems," *Journal of Polymer Materials*, vol. 62, no. 11, pp. 605–611, 2013.

[42] R. Fabris, C. W. Chow, and M. Drikas, "Evaluation of chitosan as a natural coagulant for drinking water treatment," *Water Science and Technology*, vol. 61, no. 8, pp. 2119–2128, 2010.

[43] S. J. Kim, S. J. Park, and S. I. Kim, "Swelling behavior of interpenetrating polymer network hydrogels composed of poly(vinyl alcohol) and chitosan," *Reactive & Functional Polymers*, vol. 55, no. 1, pp. 53–59, 2003.

[44] H. E. Salama, R. Gamal, and M. W. Megdy, "Synthesis, characterization and biological activity of Schiff bases based on chitosan and arylpyrazole moiety," *International Journal of Biological Macromolecules*, vol. 79, pp. 996–1003, 2015.

[45] X. Q. Yin, J. H. Chen, W. Yuan, Q. Lin, L. Jin, and F. Liu, "Preparation and antibacterial activity of Schiff bases from O-carboxymethyl chitosan and para-substituted benzaldehydes," *Polymer Bulletin*, vol. 68, no. 5, pp. 1215–1226, 2012.

[46] M. Vargas and C. Gonzalez-Martılnez, "Recent patents on food applications of chitosan," *Recent Patents on Food, Nutrition & Agriculture*, vol. 2, pp. 121–128, 2010.

[47] M. Campos, L. V. Cordi, N. Dura, and L. Mei, "Antibacterial activity of chitosan solutions for wound dressing," *Macromolecular Symposia*, vol. 245-246, no. 1, pp. 515–518, 2006.

[48] C. Cunha-Reis, A. J. El Haj, X. Yang, and Y. Ying, "Fluorescent labeling of chitosan for use in non-invasive monitoring of degradation in tissue engineering," *Journal of Tissue Engineering and Regenerative Medicine*, vol. 7, no. 1, pp. 39–50, 2013.

[49] S. P. Rwei and C. C. Lien, "Synthesis and viscoelastic characterization of sulfonated chitosan solutions," *Colloid and Polymer Science*, vol. 292, no. 4, pp. 785–795, 2014.

[50] H. Amir Afshar and A. Ghaee, "Preparation of aminated chitosan/alginate scaffold containing halloysite nanotubes with improved cell attachment," *CarbohydrPolym*, vol. 151, pp. 1120–1131, 2016.

[51] A. L. Bukzem, R. Signini, D. M. Dos Santos, L. M. Liao, and D. P. Ascheri, "Optimization of carboxymethyl chitosan synthesis using response surface methodology and desirability function," *International Journal of Biological Macromolecules*, vol. 85, pp. 615–624, 2016.

[52] S. Kumar, V. Deepak, M. Kumari, and P. K. Dutta, "Antibacterial activity of diisocyanate-modified chitosan for biomedical applications," *International Journal of Biological Macromolecules*, vol. 84, pp. 349–353, 2016.

[53] Z. Li, F. Yang, and R. Yang, "Synthesis and characterization of chitosan derivatives with dual-antibacterial functional groups," *International Journal of Biological Macromolecules*, vol. 75, pp. 378–387, 2015.

[54] M. Croce, S. Conti, C. Maake, and G. R. Patzke, "Synthesis and screening of N-acyl thiolated chitosans for antibacterial applications," *Carbohydrate Polymers*, vol. 151, pp. 1184–1192, 2016.

[55] G. V. Kumar, C. H. Su, and P. Velusamy, "Preparation and characterization of kanamycin-chitosan nanoparticles to improve the efficacy of antibacterial activity against nosocomial pathogens," *Journal of the Taiwan Institute of Chemical Engineers*, vol. 65, pp. 574–583, 2016.

[56] N. A. Mohamed and M. M. Fahmy, "Synthesis and antimicrobial activity of some novel cross-linked chitosan hydrogels," *International Journal of Molecular Sciences*, vol. 13, no. 9, pp. 11194–11209, 2012.

[57] T. M. Tamer, M. A. Hassan, A. M. Omer et al., "Antibacterial and antioxidative activity of _O_ -amine functionalized chitosan," *Carbohydrate Polymers*, vol. 169, pp. 441–450, 2017.

[58] T. M. Tamer Mohamed, A. Hassan Ahmed, M. Omer Walid et al., "Synthesis, characterization and antimicrobial evaluation of two aromatic chitosan Schiff base derivatives," *Process Biochemistry*, vol. 51, no. 10, pp. 1721–1730, 2016.

[59] W. S. W. Ngah and S. Fatinathan, "Chitosan flakes and chitosan-GLA beads for adsorption of _p_ -nitrophenol in aqueous solution," *Colloids Surf A: Physico-chemEng Aspects*, vol. 277, no. 1-3, pp. 214–222, 2006.

[60] R. Surendra Kumar, M. Moydeen, S. S. Al-Deyab, M. Aseer, and A. Idhayadhulla, "Synthesis of new morpholine _-_ connected pyrazolidine derivatives and their antimicrobial, antioxidant, and cytotoxic activities," *Bioorganic & Medicinal Chemistry Letters*, vol. 27, no. 1, pp. 66–71, 2017.

[61] S. Kumar, J. Dutta, and P. K. Dutta, "Preparation and characterization of N-heterocyclic chitosan derivative based gels for biomedical applications," *International Journal of Biological Macromolecules*, vol. 45, no. 4, pp. 330–337, 2009.